UNITED NATIONS UNIVERSITY
GEOTHERMAL TRAINING PROGRAMME
Orkustofnun, Grensasvegur 9,
IS-108 Reykjavik, Iceland

Reports 2013
Number 7

GEOTHERMAL SPACE HEATING AND THERMAL STORAGE USING PHASE CHANGE MATERIAL IN CHUMATHANG, INDIA

Vijay Chauhan
School of Engineering
Indian Institute of Technology, Mandi-175001
Himachal Pradesh
INDIA
vijay30008@gmail.com

ABSTRACT

The present work discusses utilization of geothermal energy for space heating in combination with a phase change energy storage system. The thermodynamics and thermoeconomics of the combined heating and thermal storing system were studied to show the scope of energy storage and cost savings. The analysis was done taking the second law of efficiency into consideration since the second law represents the true flow of energy. Results show the scope of utilization of phase change material for low ambient temperature conditions.

1. INTRODUCTION

Space heating has been a well-known application of geothermal energy utilization for decades. The usage of geothermal energy for space heating provides an economical and a non-polluting way for achieving human comforts. Chumathang, located in the Northwest Himalayan region, has good geothermal potential in the form of hot springs. This has also been confirmed by drilling exploration wells. The climate in the region is very cold, such that temperatures below zero are recorded during the night for almost six months of the year. Due to a lack of natural resources in the area required for the construction of houses, insulation is insufficient, thus requiring more space heating to maintain human comfort. A demonstration project for space heating has been undertaken by the Norwegian Geotechnical Institute (NGI), funded by the Research Council of Norway in collaboration with the Government of India, for heating a restaurant, which includes three rooms, in Chumathang. The project will help promote geothermal utilization for space heating on a larger scale in the area. The design for the demonstration project will also help in learning about the various factors to be considered for large scale applications since the conditions involved for the design are demanding due to local house construction and the climatic and geographical conditions prevalent in the area. The present work focuses on designing a room heating system in Chumathang. The design involves heat load calculation, equipment selection and sizing while considering the climatic conditions and the geothermal resource potential that is available.

In order to study a thermodynamic system's performance, which can either involve heating or power generation, the second law of thermodynamics plays an important role. The second law helps to better understand the energy flow processes in addition to the first law of thermodynamics. Several studies have been conducted on exergy analysis of buildings. The concept of low exergy systems for heating and cooling have been proposed in IEA ECBCS Annex 37 (2000). An exergetic life cycle assessment

for resource evaluation in the built environment was conducted by Meester et al. (2009). Shukuya and Komuro (1996) applied concepts of entropy and exergy for investigating the relationship between buildings, passive solar heating and the environment. Various results about patterns of human exergy consumption in relation to various heating and cooling systems were given by Saito and Sukaya (2001). Conclusions about the inadequacy of the concept of energy conservation in understanding important aspects of energy utilization processes were made by Yildiz and Gungör (2009). The second law analysis is important in order to have an efficient utilization of the available resource.

It is a well-known fact that thermal heating systems have low second law efficiency. In geothermal systems, water exiting after passing through heat exchangers and radiators still has sufficient exergy required for human comfort and could be stored for off peak requirements. Another important concern about storage is when available flow rate is limited and heat requirements are high. Saving energy during off peak heating can help to fulfil the peak load requirements. Such applications are practiced well with other renewable energy sources such as solar energy. The application of energy storage in geothermal energy utilization can also help reduce the major capital investment required for drilling purposes. The present work focuses on the application of energy storage systems in geothermal energy utilization. Thermodynamic analysis was done for a geothermal heating system in combination with phase change material storage added parallel to the geothermal exit flow from a heat exchanger for making efficient utilization of geothermal energy. Exergoeconomic analysis of the combined heating and storage was also done in order to find the scope of cost savings.

1.1 Chumathang geothermal field

Chumathang is located in the Ladakh district of Jammu and Kashmir State of India. The place is situated across the Northwest Himalayan range along the banks of the Indus River and at an altitude of 4300 m above mean sea level. A thick sequence of shallow marine to fluvial sediments deposited over a granitic basement is found in the area. Chumathang field is located in this belt. Spring deposits in the form of carbonate plateaus can be found in the area. Thermal manifestations can be seen on the northern bank of the river in an area of about 1 square kilometre. The area has around 73 hot springs with a discharge of about 200 litres per minute and a temperature range varying from 30 to 87°C (Razdan et al., 2008).

Geochemistry
The pH value of the water in Chumathang field ranges from 6.9 to 8.6. The water has high SO_4 concentration and low Cl, Na, HCO_3 and K. The fluid is classified as sodium bicarbonate and sulphate type. The base temperatures calculated using Na-K, Na-K-Ca and SiO_2 thermometry are found to be 145-166°C, 160-184°C and 148-174°C, respectively.

1.2 Houses in Chumathang

Figure 1 shows the general construction of a house in Chumathang, which is constrained by limited local resources. A common house has three floors. The ground floor walls are made of stone and the upper floor walls are comprised of sun dried mud bricks plastered with clay. The roofs are constructed from poplar beams, willow branches, mud and earth. Roofs are flat as there is little rain and snow can be removed easily. Grass is piled on the roof over walls to protect from precipitation.

FIGURE 1: A house in Chumathang

The above mentioned materials used for construction makes houses in Chumathang less insulated than normal houses. The cold climate lasts for more than half of the year, adding to high heat losses from the houses.

1.3 Weather analysis

The heat load of a building mainly depends upon the outdoor ambient temperature. The other factors influencing heat load are wind velocity and solar radiation. Figure 2 shows the monthly average, minimum and maximum temperature in the Chumathang region. The figure shows that the outside maximum temperature reaches the room temperature required for human comfort, 20°C, only one month in a year. Temperatures below zero prevail in the area for more than six months a year, reflecting the requirement for space heating in the region.

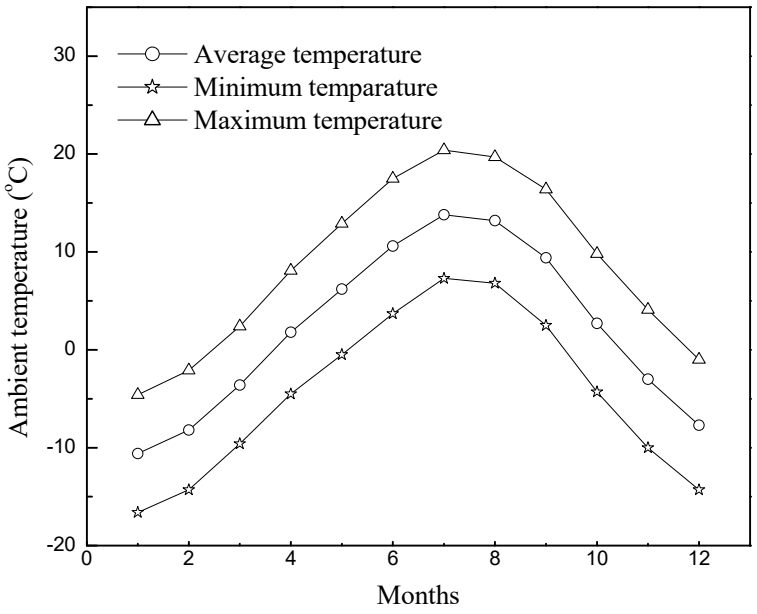

FIGURE 2: Monthly outdoor temperature in Chumathang

1.4 Phase change material (PCM)

One of the best solutions for the problem when demand and supply are out of phase is the use of energy storage materials. The key to effective utilization of alternative energy sources is efficient and economical energy storage systems. Energy storage systems which are currently being researched by the scientific community are mainly of three types, classified on the basis of the principle under which they work. The first one consists of an energy storage system utilizing chemical heat reaction for absorbing and emitting heat energy. The second class of storage devices is that of utilizing sensible heat capacity for storage such as storing in tanks. The third and most useful energy storage system utilizes phase change materials (PCM). Such systems absorb and release heat energy as latent heat of the storing material with a change of phase. Various advantages of PCM over other storage systems have emphasized its importance over the years. The studies done by Adebiyi and Russell (1987) concluded two advantages derived from using a phase change material in a thermal energy storage system design. The first advantage was an increase in the second law of efficiency of the system as compared to the one using sensible heat storage system. The second major advantage was the reduced amount of storage material required. Since PCM is based on the principle of storing heat as latent energy of phase change, the energy stored is far higher than that stored by sensible heating systems which store energy according to their specific heat capacity.

Analysis of latent heat storage based on the first law of thermodynamics can be found in various literatures. The first law analysis helps us to obtain a workable design but not an optimum one. In order to consider the effects of time and the temperature at which heat is supplied, analysis of the second law is required. According to Bejan et al. (1996) an optimal system which a designer can develop, having the least irreversibility, is based on minimization of entropy generation. The application of second law analysis for studying latent heat storage was studied by Bjurstrom and Carlsson, 1985; Adebiyi and Russell, 1987; and later by Bejan (1996). A study (El-Dessouky and Al-Juwayhel, 1997) was done for investigating the effects of different variables on the entropy generation number defined by Bejan (1996). The analysis considered the case of storage material exchanging heat at a constant melting point. Two commonly available storing materials, paraffin wax and calcium chloride, were considered with air or water as the heating fluid.

A number of materials exist which can be used as PCM over a wide range of temperatures. A list of such materials can be found in the literature (Abhat, 1983). The selection of a PCM for energy storage

is based on the fulfilment of criteria such as high latent heat capacity, non-corrosiveness, high thermal conductivity, and it should be non-toxic, without deposition or super cooling. The transition temperature of the phase change material is decided by the room temperature required.

1.5 Importance of PCM to geothermal energy storage

Studies on the analysis of PCM, both numerical and experimental, have been reported in the literature (Farid et al., 2004). The work is mainly focused on the relationship to solar energy storage. The present work proposes the use of PCM for storage of geothermal energy used for direct heating applications. It is important to know how the stored geothermal energy will be utilized when the mass flow itself can be controlled. The answer depends upon the conditions for storage application. For an existing heating system using radiators and heat exchangers, an important fact also discussed in literature is the variation of geothermal exit temperature with outside ambient temperature for a fixed design network (Karlsson and Ragnarsson, 1995). It is found that as the ambient temperature decreases, the exit temperature of a geothermal heating network increases. The increase in exit temperature reflects an increase in useful heat loss. In terms of the second law of efficiency, the decrease in ambient temperature causes an increase in exergy loss to the atmosphere. Surely the application of energy storage can provide a means of saving energy which can be used in the off peak time when demand is low. Stored heat from the geothermal exit fluid at night can be used for fulfilling daytime requirements. The other advantage of thermal storage for geothermal application is found in areas with limited flow and high heat demand. Heat energy in such cases could be stored during off peak or daytime and utilized for peak load demands during the night.

The advantage of PCM over a sensible storage system is the low volume requirement of the storage material. Since the latent heat of PCM is generally many times greater than the specific heat of water, it requires far less space for storage than for storing water. Another advantage of PCM is its ability to absorb and release heat at a constant temperature. This is not possible in storing heat using sensible heating, and heat loses its quality with time as temperature decreases. The PCM, on the other hand, provides constant temperature heating.

1.6 Thermoeconomics

Thermoeconomic or exergoeconomic analysis considers both thermodynamic and economic principles for improving system performance. Exergoeconomic analysis helps in quantifying the exergy losses in terms of monetary losses. According to Bejan et al. (1996) thermoeconomics is defined as the branch of engineering that combines exergy analysis and economic principles to provide the system designer or operator with information not available through conventional energy analysis and economic evaluations, but crucial to the design and operation of the cost effective system. Exergetic cost analysis for space heating using a ground source heat pump system was done by Jingyana et al. (2010). The work shows the sensitivity of various sub systems to unit exergy cost. Application of exergoeconomic analysis for geothermal district heating systems was presented by Oktay and Dincer (2009) and reviewed by Hepbasli (2010) using energy, exergy and economic aspects. The effect of reference temperature on the thermoeconomic evaluation of geothermal heating system was studied by Keçebaş (2013).

For making economical use of a thermodynamic system, attention should be given to the cost paid for inefficiencies. The calculation of such costs helps in governing the final cost of the product in addition to improving the effectiveness of the system. The economic costs required for thermoeconomic analysis are obtained from relationships which represent cost as a function of design and geometrical parameters such as length and volume.

2. HEAT LOAD CALCULATION

Several different tools for evaluating the performance of a building's heat load exist (Crawley et al., 2008). Many parameters about the geometry, thermo-physical properties and construction are required in order to make use of these simulation tools for evaluating building performance. For evaluating the energy consumption of a building, envelope parameters and air changes are the major parameters to be evaluated (Budaiwi, 2011). Comparison of different existing methods for building calculation was done by Carlos and Nepomuceno (2004) focusing on the energy use of space heating for a standard case. A simplified model for calculating the heat load was also proposed in the paper. The model used fewer input parameters and required little time for making calculations. Comparison of the simplified model with pre-existing models gave good similar results.

The present work makes use of the model proposed by Carlos and Nepomuceno (2004) for heat load calculation for the application required. The input parameters required for the heat load calculation were in accordance with the existing conditions and requirements. For the present analysis, steady state conditions were assumed. Also the internal conditions were assumed to be constant and the effects of solar radiation on the building neglected. The approach for calculating the heat load requirement is described as follows:

Overall heat transfer coefficient

The overall heat transfer coefficient U (W/m^2 K) is calculated as (for definitions see Nomenclature):

$$\frac{1}{U} = \frac{1}{h_{int}} + \frac{x}{\lambda_{surf}} + \frac{1}{h_{ext}} \tag{1}$$

The wall has the thickness x (m) and thermal conductivity λ_{surf} (W/mK). The value of the heat transfer coefficient h_{int} (W/m^2 K) of the inside wall is assumed constant, equal to 8.The convective heat coefficient outside the wall, h_{ext} (W/m^2 K), is calculated as given by Mirsadeghi et al. (2013):

Windward side:

$$h_{ext} = 8.07 \times V_w^{0.605} \tag{2}$$

Leeward side:

$$h_{ext} = 18.64 \times (0.3{+}0.05V_w)^{0.605} \tag{3}$$

where V_w = Wind velocity in m/s (assumed 10 m/s).

Building heat loss

Transmission heat loss:

$$Q_{transmission} = U \times A_{exp} \times \Delta T \tag{4}$$

Ventilation heat loss:

$$Q_{ventilation} = \frac{C_a \times \rho_a \times Volume \times air\ changes/hour \times \Delta T}{3600} \tag{5}$$

where $\Delta T = T_{room} - T_{amb}$.

Total heat loss:

$$Q_{loss} = Q_{transmission} + Q_{ventilation} \tag{6}$$

Internal heat gain

The internal heat gain occurs from the occupants and the heat emitting objects in a room. Since the number of occupants and objects varies, the heat gain is calculated from an estimated heat gain per floor area:

$$Q_{gain} = \nu \times A_{floor} \tag{7}$$

where ν = Heat gained per unit floor area, assumed to be 4 W/m^2.

Seasonal useful heat gain:

$$Q_u = \eta Q_{gain} \tag{8}$$

where η = Utilization factor for the heat gain.

The utilization factor is used for taking the thermal inertia of a building into account. For the calculation of the utilization factor, different factors need to be calculated as follows.

The ratio of heat gain and heat loss given as:

$$\phi = \frac{Q_{gain}}{Q_{loss}} \tag{9}$$

Time constant of the building in seconds given as:

$$Z = \frac{K}{H} \tag{10}$$

where K = Internal heat capacity of building (J/K); and
H = Coefficient for the heat loss through ventilation and transmission (W/K).

For easy calculation, the time constant for different building compositions was adapted from Kalema and Pylsy (2008).

The utilization factor can be found as:

$$\eta = \frac{1 - \phi^n}{1 - \phi^{n+1}} \quad if\ \phi \neq 1 \tag{11}$$

$$\eta = \frac{\phi}{\phi + 1} \quad if\ \phi = 1 \tag{12}$$

The value of n in the above equation depends on the time constant given as:

$$n = n_o + \frac{Z}{Z_o} \tag{13}$$

The value of parameter n_o is 1 if the calculation is made on a monthly basis and 0.8 for a seasonal basis. Z_o is the reference time constant having a value of 16 hours for monthly calculation and 28 hours for seasonal calculation.

Upon obtaining all the above parameters for a building, the net heat load can be found as:

$$Q = Q_{loss} - \eta Q_{gain} \tag{14}$$

Results of heat load calculation are given in Section 5.

3. THERMODYNAMIC MODELLING

Figure 3 shows the schematic diagram of the combined space heating and thermal storage system. The geothermal water is first passed through a heat exchanger giving heat to the secondary fluid. The secondary fluid passes through the radiator heating system giving heat to the room and then returns to the heat exchanger, forming a closed loop. The geothermal fluid, after exiting the heat exchanger, passes

into a phase change thermal storage system. The geothermal fluid gives heat to the phase change material and then exits the system. Thermodynamic modelling of the combined system is described below:

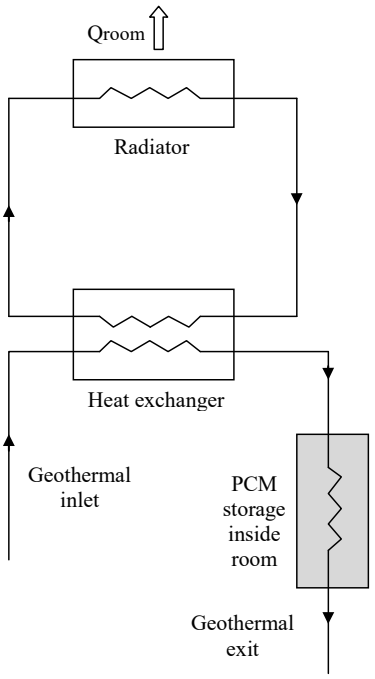

FIGURE 3: Schematic diagram of combined heating and storing system

3.1 Heating system

Space heating using geothermal fluid is generally done using one of two methods, by sending geothermal fluid directly through space heating radiators or by using a heat exchanger which transfers heat from the geothermal fluid to the secondary fluid which then passes through the radiators for giving heat. Where geothermal fluid is unsuitable for direct use, the latter technique is applied. Also for cases where the minimum ambient temperature goes below the freezing point of water, anti-freeze is used in the secondary loop.

The present analysis assumes use of the indirect method of space heating such that the geothermal fluid gives heat to the secondary fluid which is passed through radiators for room heating. The radiators are designed for fixed design conditions at assumed room temperature. For ambient temperatures other than the design temperature, the heat load is calculated as:

$$\dot{Q}_T = \dot{Q}_{des}\left(\frac{T_{amb} - T_{room}}{T_{des} - T_{room}}\right) \tag{15}$$

The amount of heat transferred from a radiator is given as:

$$\dot{Q}_T = A_R \times U_R \times LMTD_R \tag{16}$$

The value of the logarithmic mean temperature difference between the radiator and the room air can be found using the following relationship:

$$LMTD_R = \frac{T_{R,in} - T_{R,out}}{ln\left(\frac{T_{R,in} - T_{room}}{T_{R,out} - T_{room}}\right)} \tag{17}$$

It is found from experience that the logarithmic mean temperature difference varies with the radiator heat load as follows:

$$\frac{\dot{Q}_T}{\dot{Q}_{des}} = \left(\frac{LMTD_R}{LMTD_{R,des}}\right)^n \tag{18}$$

The value of exponent *n* is 1.3 (Anon, 1977).

Combining Equations 17 and 18, the radiator exit temperature can be found for a heat load other than the design load. Since the combined equation is an implicit function of the radiator exit temperature, any numerical technique such as the Newton Raphson method can be used for solving the equation.

On obtaining the temperature at the radiator outlet, the mass flow rate of fluid required through the radiator is given as:

$$\dot{m}_{rad} = \frac{\dot{Q}_T}{C_{R,f}\left(T_{R,in} - T_{R,out}\right)} \tag{19}$$

The calculation of the above parameters for radiators requires full definition of the radiator side parameters. The output parameters from the radiator and the geothermal fluid inlet parameters (flow

rate and temperature), are the input parameters for the heat exchanger. In general, plate type heat exchangers are used for residential heating due to the advantages of low heating space, high heat transfer rate and ease in construction and maintenance over shell and tube type heat exchangers. With limited information for calculation of heat transfer coefficients through plate heat exchangers, the present analysis uses the relationship suggested by Incropera et al. (2007) for flow through circular pipes with diameter equal to the hydraulic diameter of a non-circular channel of the heat exchanger through which geothermal and secondary fluid passes. The relationship is given as:

$$Nu = 0.0296\, Re^{0.8} Pr^{0.333} \tag{20}$$

where Nu = Dimensionless Nusselt number;
Pr = Dimensionless Prandtl number; and
Re = Dimensionless Reynolds number.

The Nusselt number and the Reynolds number are calculated as:

$$Nu = \frac{hD_h}{\lambda_f} \tag{21}$$

$$Re = \frac{\rho_f v_f D_h}{\mu_f} \tag{22}$$

The value of the Prandtl number (Pr) can be found from literature as a material property at different temperatures.

On finding the values of the heat transfer coefficient for both geothermal water and radiator fluid, the overall heat transfer coefficient for the heat exchanger is found as follows:

$$\frac{1}{U_{HX}} = \frac{1}{h_g} + \frac{x_{HX}}{\lambda_{HX}} + \frac{1}{h_R} + R_{HX} \tag{23}$$

The amount of heat transferred through the heat exchanger is given as:

$$\dot{Q}_T = A_{HX} \times U_{HX} \times LMTD_{HX} \tag{24}$$

Knowing the value of the heat exchange required and the area for which the heat exchanger is selected for a specific design, the logarithmic mean temperature difference of the heat exchanger can be calculated from the above equation. The geothermal exit temperature from the heat exchanger can then be calculated from the following equation:

$$LMTD_H = \frac{\left(T_{g,in} - T_{R,in}\right) - \left(T_{g,out} - T_{R,out}\right)}{ln\left(\frac{T_{g,in} - T_{R,in}}{T_{g,out} - T_{R,out}}\right)} \tag{25}$$

The above equation signifies the logarithmic mean temperature difference as an implicit function of geothermal water return temperature; hence, it needs to be solved numerically. Knowing the return water temperature, the mass flow rate of the geothermal fluid can then be found as:

$$\dot{m}_{geo} = \frac{\dot{Q}_T}{C_{g,f}\left(T_{g,in} - T_{g,out}\right)} \tag{26}$$

3.2 Phase change material

The present work focuses on the analysis of PCM combined with a geothermal space heating system. The aim of the study is to calculate the amount of energy and exergy saved using PCM combined with geothermal space heating. The amount of PCM to be used for thermal storage depends upon the building heat load requirement and the difference in ambient temperature during storage and discharging. Since

the ambient temperature difference varies from season to season, the analysis assumed the mass phase change material to be 400 kg. The storage material mass and other physical properties were kept constant during the analysis. The heat storage system was assumed to consist of two concentric cylinders with inner and outer diameter of 0.02 and 0.045 m such that the heat source fluid flowed through the inner periphery and the storage material was filled between the cylinders as shown in Figure 4. The calculated length required for storage was found to be 186 m.

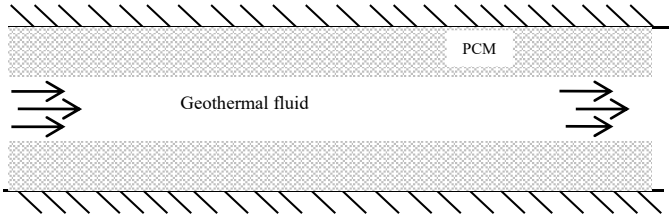

FIGURE 4: Configuration of thermal storage system

The PCM material used was calcium chloride. The properties of the PCM material and the heating fluid, water, were taken from El-Dessouky and Al-Juwayhel (1997). Analysis for the PCM, using air and water as the heating fluid, was discussed in the corresponding literature, considering water and air as the ideal fluid. For calculation of exergy terms, this assumption did not validate fully for water. Another important exergy analysis for phase change material was done by Bjurstrom and Carlsson (1985). Relations were derived for the amount of exergy stored in PCM and the final temperature of storage material. The present work uses the equations derived in Bjurstrom and Carlsson (1985) for analysing the system. The assumptions used in the analysis are:

- There is no heat exchange between the storage system and the surroundings during the charging process;
- The heat exchanger wall is assumed to have no resistance to heat transfer;
- Thermophysical properties of PCM and flowing fluid are assumed to be constant; and
- Since the analysis was done using phase change material with low transition temperature, the temperature difference between the transition temperature and the room temperature was small, hence all stored exergy was assumed to be used for room heating.

The heat transfer coefficient, h_f, between the heat transfer fluid and the wall is calculated from Equation 21. For turbulent flow, Equation 20 is used to obtain the Nusselt number, whereas for laminar flow $Nu = 3.66$.

The heat transfer coefficient between the wall and the storage material were calculated according to the relationships developed by Yanadori and Masuda (1989), based on experimental data.

$$h_m = \frac{2\lambda_s}{0.4\left(D_{inner} ln\left(\frac{D_{outer}}{D_{inner}}\right)\right)} \tag{27}$$

After obtaining the convective heat coefficient for the geothermal fluid and the phase change material, the overall heat transfer coefficient for PCM storage is calculated as:

$$\frac{1}{U_s} = \frac{1}{h_f} + \frac{1}{h_m} \tag{28}$$

In the above equation, resistance due to the wall is neglected as it is small in comparison to the convective heat transfer coefficients.

When the available information for calculating the heat transfer is insufficient, the Number of Transfer Units is used. This method helps to calculate heat transfer when all the inlet and exit temperatures are not given. The Number of Transfer Units on the fluid side is given by:

$$NTU = \frac{U_s \pi D_{inner} L_s}{\dot{m}_{geo} c_{g,f}} \tag{29}$$

For analysis, the initial temperature of the storage material and the inlet temperature of the heat source are assumed. The procedure used for calculating the final storage temperature and the amount of exergy stored is found from equations given by Bjurstrom and Carlsson (1985), as follows:

A dimensionless time Ω is defined as:

$$\Omega = \frac{\dot{m}_{geo} c_{g,f}}{M_{pcm} C_{pcm}} t \tag{30}$$

For analysis, temperatures are made dimensionless using the following equation:

$$\theta = \frac{T - T_o}{T_o} \tag{31}$$

The temperature efficiency (*r*) of the heat exchanger is given as:

$$r = 1 - \exp(-NTU) \tag{32}$$

The phase change material exhibits three stages of heat absorption: (1) sensible heat in solid phase from initial temperature to transition stage; (2) Latent heat during transition phase, and (3) Sensible heat in liquid phase. An equivalent heat capacity C_{pcm} is defined by the relationship:

$$M_{pcm} C_{pcm} (T_l - T_b) = M_{pcm} C_s (T_m - T_b) + M_{pcm} H + M_{pcm} C_l (T_l - T_m) \tag{33}$$

or

$$\theta_l - \theta_b = \alpha(\theta_m - \theta_b) + \omega(\theta_l - \theta_b) + \sigma(\theta_l - \theta_m) \tag{34}$$

The constants α, ω and σ are given as:

$$\alpha = \frac{C_s}{C_{pcm}} \tag{35}$$

$$\omega = \frac{H}{C_{pcm}(T_l - T_b)} \tag{36}$$

$$\sigma = \frac{C_l}{C_{pcm}} \tag{37}$$

For heating at a temperature below the phase transition temperature, the instantaneous storage temperature as a function of time is given as:

$$\theta_s = \theta_b + (\theta_i - \theta_b)\left(1 - exp^{-r\Omega'}\right) \tag{38}$$

where Ω' is given as:

$$\Omega' = \frac{\Omega}{\alpha} \tag{39}$$

For heating the PCM above the transition temperature, the equations for instantaneous storage temperature and geothermal fluid outlet temperature are given as:

$$\theta_s = \theta_m + (\theta_i - \theta_m)\left(1 - exp^{-r\Omega''}\right) \tag{40}$$

$$\theta_e = \theta_i(1 - r) + \theta_m r \tag{41}$$

where Ω'' is given as:

$$\Omega'' = \frac{1}{\sigma}\left(\theta - \left(\frac{\alpha}{r} ln\left(\frac{\theta_i - \theta_b}{\theta_i - \theta_m}\right)\right) - \frac{\omega}{r}\left(\frac{\theta_l - \theta_b}{\theta_i - \theta_m}\right)\right) \tag{42}$$

The second and third terms in the parenthesis representing the dimensionless times required for bringing PCM to phase transition temperature and its completion.

For PCM where the storage temperature exceeds the transition temperature, the amount of energy stored in PCM is given by:

$$Q_{stored} = M_{pcm}C_s(\theta_m - \theta_b) + M_{pcm}H + M_{pcm}C_l(\theta_s - \theta_m) \quad (43)$$

Discharging

The phase change material storage is the cylindrical tanks or heat exchanger having phase change material in the annulus and hot water flowing inside. Such an arrangement can act as a radiator when placed in a room. The discharging of heat, stored during the night when the geothermal flow rate and temperature to phase change inlet is high, takes place during the daytime. As the daytime heat load requirement in rooms is low, the mass flow rate of the geothermal fluid is less and the inlet temperature of the geothermal fluid is low. Stopping the flow of geothermal water through phase change material makes the phase change storage system start to discharge heat since the phase change storage temperature is higher than the room temperature. The phase change storage system initially discharges heat at a higher rate since the initial storage temperature is much higher than the room temperature. On reaching the transition temperature, the phase change material gives heat at a constant rate because of a constant storage temperature equal to the phase change transition temperature. The low value of the convective heat transfer coefficient between the storage wall and the room does not permit the storage system to lose heat fast, hence allowing a longer period of discharge.

4. SYSTEM ANALYSIS

4.1 Exergy analysis

4.1.1 Room envelope system

On determining the total heat load for the room, the amount of exergy required for the heat load is determined. In order to determine the exergy required, the quality factor of the room air must be estimated. The quality factor describes the maximum energy that can be converted into useful work. Since heat energy is a form of low grade energy, the amount of exergy present in the heat energy is determined by the quality factor which is estimated by means of the Carnot efficiency, given as:

$$Y_{q,room} = 1 - \frac{T_{amb}}{T_{room}} \quad (44)$$

The amount of exergy required for satisfying the heat load demand is given as:

$$\dot{\mathcal{E}}_{room} = Y_{q,room} \times \dot{Q}_T \quad (45)$$

4.1.2 Heating system

The radiator system is used for heating the room. In order to calculate the exergy load of the radiator system, the inlet and outlet temperatures of the system play important roles. The radiator surface temperature is calculated as the logarithmic mean temperature of the emission system as defined by Moran and Shapiro (1998):

$$T_{rad} = T_{room} + \frac{1}{2}\left(\frac{T_{R,in} - T_{R,out}}{ln\left(\frac{T_{R,in} - T_{room}}{T_{R,out} - T_{room}}\right)}\right) \quad (46)$$

The amount of exergy given by the radiator is then given as:

$$\dot{\mathcal{E}}_{rad} = \dot{Q}_T \left(1 - \frac{T_{amb}}{T_{rad}}\right) \tag{47}$$

In order to calculate exergy changes in a component along a flow line, the exergy flow rate at point *i* is calculated using the equation given by Bejan et al. (1996):

$$\dot{\varepsilon}_i = \dot{m}_{in}[(h_{in} - h_o) - T_o(s_{in} - s_o)] \tag{48}$$

The values of enthalpy and entropy of the heating and radiator fluid as a function of temperature and pressure are calculated using the relationships given by Cooper and Dooley (2007).

The amount of exergy given by the geothermal fluid is calculated as:

$$\dot{\varepsilon}_{geo} = \dot{m}_{geo}\left[\left(h_{geo,in} - h_o\right) - T_{amb}\left(s_{geo,in} - s_o\right)\right] \tag{49}$$

4.1.3 Storage system

The amount of exergy stored in the PCM is given by Bjurstrom and Carlsson (1985) as:

$$\begin{aligned}\varepsilon_{stored} = M_p C_{pcm} T_{amb} \Bigg\{ & \alpha \left[(\theta_m - \theta_b) - ln\left(\frac{1+\theta_m}{1+\theta_b}\right)\right] + \omega(\theta_l - \theta_b)\frac{\theta_m}{1+\theta_m} \\ & + \sigma\left[(\theta_s - \theta_m) - ln\left(\frac{1+\theta_s}{1+\theta_m}\right)\right]\Bigg\}\end{aligned} \tag{50}$$

4.2 Piping system design and pump selection

Design of the piping system requires the integration of mechanical, thermal and economic aspects. The material used for a pipe system depends upon the fluid flowing through it. Fluid conditions such as high temperature, high pressure, corrosive and hazardous are some of the factors that need to be taken into account while selecting pipe material. For applications requiring hot fluid to flow through pipes, thermal expansion should be taken into consideration.

Head loss
The head loss in a pipe due to friction is calculated using the Bernoulli equation. It can be estimated using the following equation:

$$h_l = \frac{4 f L_p {v_f}^2}{2 g D_p} + k\frac{{v_f}^2}{2} \tag{51}$$

where the first term represents head loss due to pipe friction and the second term represents head loss due to bending and resistance.

The value of the factor for different fittings, *k,* can be found from the table given in Bejan et al. (1996). The factor *f* represents the Fanning friction factor. The value of the Fanning friction factor is a function of the Reynolds Number and pipe roughness and is given as:

$$\frac{1}{\sqrt{f}} = -4log\left(\frac{e_p/D_p}{3.7} + \frac{1.256}{(\sqrt{f})Re}\right) \tag{52}$$

The above implicit function can be solved using a numerical technique to obtain the value of the friction factor.
On knowing the head loss through the pipe and the required head, the pump power requirement is calculated as:

$$P_{pump} = \frac{\dot{m}_f g(h_l + h_s)}{\eta_{pump}} \times 100 \tag{53}$$

Pipe selection
Various types of pipe materials exist with varying costs and durability. Different types of pipe materials used for geothermal applications include: various types of steel, polyvinyl, polybutylene, polyethylene and fibre glass. In addition to cost, temperature and the chemical properties of the geothermal fluid decide the type of pipeline material to be used.

For pipes carrying geothermal fluid for longer distances, some form of insulation is required. The insulation can be provided by using a pre insulating piping system, field applied methods or backfill methods. A pipe having a pre insulating system will have an insulation layer covering the carrier pipe. Many different combinations of insulation jacket and carrier pipe materials are available in the market, the most common using polyurethane as an insulation material. Almost 50% of the distribution cost is associated with pipe insulation. Much of the pipe cost can be saved by using uninsulated pipes. The heat loss due to no insulation is compensated for by increasing the flow rate of the fluid.

4.3 Exergoeconomic analysis

The exergy transformation process in a system is represented in Figure 5. The total exergy given to a system includes fuel exergy which is transformed into product exergy, some part of which includes exergy destruction and exergy loss. The increase in efficiency causes an increase in exergy output for a given input but also causes an increase in the costs required to improve the system.

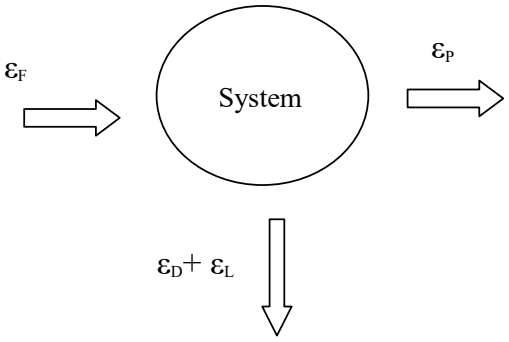

FIGURE 5: Exergy flow in a system

For exergoeconomic analysis, cost is assigned for every exergy flow in a system. The cost is proportional to the amount of exergy the flow contains. The product cost is defined according to the fuel cost, capital expenditure and other operating and maintenance costs required for production or services. The general equation is given as:

$$\dot{C}_p = \dot{C}_F + \dot{Z}^{Cl} + \dot{Z}^{OM} \tag{54}$$

The equation signifies that the total cost associated with the product is the sum of the fuel cost, capital investment and the other costs related to the operation and maintenance of the system producing the product.

A general cost balance equation in terms of cost per unit exergy for an i^{th} component having heat and work interaction with the surroundings can be represented in terms of costs per unit exergy:

$$\sum(c_{out,i}\dot{\varepsilon}_{out,i} + c_{w,i}\dot{W}_i) = \sum(c_{in,i}\dot{\varepsilon}_{in,i} + c_{Q,i}\dot{\varepsilon}_{Q,i} + \dot{Z}_i^{Cl} + \dot{Z}_i^{OM}) \tag{55}$$

The inlet cost in the above equation is obtained from that of the exit cost of the previous component. For the first component, the inlet cost is the cost at which the fuel is supplied. Hence, the above equation can be solved for the unknowns.

4.3.1 Purchase equipment cost

For real life applications, equipment cost can be obtained from a vendor's catalogue. Generally it is not possible to obtain detailed costs of every component for every design condition. For such cases, the literature provides some useful sources. Mathematical charts and relationships built from past experiences are available giving cost values in terms of different parameters such as design and geometry. The simplest way for estimating product cost is by using an exponential law which defines the product cost as an exponential function of the size of the component. The relationship is given as follows:

$$I = I_r \left(\frac{S}{S_r}\right)^e \tag{56}$$

Such a relationship is assumed to be valid for a given range of equipment sizes. A general sixth-tenth rule is used for any equipment by taking the value of exponent to be 0.6. Different values of reference costs and their size along with the type of component are given by Boehm (1987).

Because of various economic factors, the cost always changes with time. The above relationship is for finding the cost with the reference cost of the indexed year. The obtained cost is brought to the current year cost by using the conversion relationship given as:

$$Reference\ year\ cost = Original\ cost \times \frac{Reference\ year\ cost\ index}{Cost\ index\ for\ year\ for\ which\ calculation\ was\ made} \tag{57}$$

The cost index used in the above equation takes into consideration inflation in the cost of the material, equipment and labour. Various cost indices are available in the literature. The present analysis uses Marshall et al. (2009) for indexing the equipment cost. The exergoeconomic analysis requires levelized costs of the equipments. For converting investment cost into levelized costs, a Capital Recovery Factor (CRF) is used, given by following equation:

$$CRF = \left(\frac{i(1+i)^N}{(1+i)^N - 1}\right) \tag{58}$$

The other factor to be taken into consideration while calculating component cost is operation and maintenance cost. The analysis assumes an annual 2% of the investment cost of each component as the operation and maintenance cost (β). The total cost flow rate associated with the component a with t hours of annual operation is then calculated as:

$$\dot{Z}_i = \frac{I_i(CRF + \beta)}{t \times 3600} \tag{59}$$

4.3.2 Exergy costs

Guidelines for obtaining equations for different streams can be found in the literature (Bejan et al., 1996). The present case mainly involves the usage of heat exchanging components. The balancing equations for the components used are described as:

Heat exchanger
In this system a heat exchanger is used to deliver heat coming from a geothermal inlet stream to a radiator exit stream which is the product stream. Hence, the following equations are obtained:

$$\dot{C}_{g,in} - \dot{C}_{HX,out} + \dot{C}_{R,out} - \dot{C}_{R,in} = -\dot{Z}_{HX} \tag{60}$$

Also, since the fuel side is that of the geothermal stream, its cost per unit exergy remains constant. The equation is given as:

$$\frac{\dot{C}_{g,in}}{\dot{\mathcal{E}}_{g,in}} = \frac{\dot{C}_{HX,out}}{\dot{\mathcal{E}}_{HX,out}} \tag{61}$$

Radiator
The cost associated with the radiator is charged to the product which is the exergy flowing out from the radiator for room heating. The equation obtained is:

$$\dot{C}_{R,in} - \dot{C}_{R,out} - \dot{C}_{heating} = -\dot{Z}_R \tag{62}$$

Also, no exergy is added to the inlet stream, hence the cost per unit exergy remains the same; the equation obtained is:

$$\frac{\dot{C}_{R,in}}{\dot{\varepsilon}_{R,in}} = \frac{\dot{C}_{R,out}}{\dot{\varepsilon}_{R,out}} \tag{63}$$

Storage system

The cost associated with storage is charged to the product, which is the exergy stored in the system. The equation obtained is:

$$\dot{C}_{HX,in} - \dot{C}_{g,out} - \dot{C}_{storage} = -\dot{Z}_{storage} \tag{64}$$

Also, no exergy is added to the inlet stream, hence the cost per unit exergy remains the same; the equation obtained is:

$$\frac{\dot{C}_{HX,out}}{\dot{\varepsilon}_{HX,out}} = \frac{\dot{C}_{g,out}}{\dot{\varepsilon}_{g,out}} \tag{65}$$

The above linear equations can be solved simultaneously to obtain the unknown variables.

5. RESULTS AND DISCUSSIONS

5.1 Heating system design

Tables 1 and 2 show the overall heat transfer coefficient for the different structures of room and restaurant. The calculation assumes that the larger side of the rooms is the windward side. Since the restaurant is surrounded by other building on three sides, only the glass window side is assumed to be the windward side.

TABLE 1: Overall heat transfer coefficient for rooms

Wall (windward)	3.1 W/m^{2}K
Wall (leeward)	2.8 W/m^{2}K
Glass	6.1 W/m^{2}K
Door	1.7 W/m^{2}K
Roof	4.1 W/m^{2}K
Floor	0.56 W/m^{2}K

TABLE 2: Overall heat transfer coefficient for restaurant

Wall (leeward)	2.8 W/m^{2}K
Glass	6.1 W/m^{2}K
Door	1.7 W/m^{2}K
Roof	4.1 W/m^{2}K
Floor	0.5 W/m^{2}K

The proposed system was analysed for variable radiator inlet temperature at different ambient conditions. The design conditions for the heating system assumes -15°C ambient temperature and 20°C room temperature. The fluid used in the secondary loop was assumed to be water. Table 3 shows the values of the different variables for the geothermal heating system.

TABLE 3: Design parameters and their values

Parameter	Value
Q_{load}	34.2 kW
$\dot{m}_{geo}$	0.25 kg/s
$\dot{m}_{rad}$	0.25 kg/s
$T_{R,in}$	75.0°C
$T_{R,out}$	42.5°C
$T_{g,in}$	80.0°C
$T_{g,out}$	47.5°C

Radiator

Different sizes of radiators can be selected from the manufacturer's catalogue depending upon the heat load requirement and the space available for installation. The catalogue specifies the radiator size and power output for particular models for given logarithmic temperature differences of the radiator and room temperature. Correction factors are available in the catalogue for getting heat output at other logarithmic temperature differences for a selected model. For the present design, radiators with a 40° logarithmic mean temperature difference design were selected, supplied by BYKO. The radiator models selected are given in Table 4.

TABLE 4: Radiator selection

Building	Required heat load (kW)	Model	No of radiators	Radiator heat capacity (kW)	Size
Rooms	11.43	E-33	3	3.85	0.6 m × 2.0 m
Restaurant	22.67	E-33	4	3.96	0.4 m × 2.8 m
		E-33	3	2.29	0.3 m × 2.0 m

Heat exchanger

For geothermal heating, generally plate type heat exchangers are preferred. The plate type heat exchangers offer many advantages over other types of heat exchangers. The nominal approach temperature of plate type heat exchangers is less than for other heat exchangers. In addition, the overall heat transfer coefficient of plate type heat exchangers is three to four times higher than shell and tube units. The construction of plate type heat exchangers makes them easier to maintain also. The plate type heat exchangers also permit expansion by the addition of extra plates as required. In addition, the compactness of the plate type heat exchangers also adds to its preference for selection.

TABLE 5: Heat Exchanger Specifications

Plate material	Stainless steel type AISI 316
Heat capacity	35 kW
Plate thickness	0.00035 m
Fouling Factor	0.075 m^2 K/kW
Thermal conductivity	15.0 W/mK
Plate spacing	0.002 m
Plate width	0.1 m
Number of plates	81
Heat transfer area/plate	0.025 m^2

For the present heat load requirement, a 4/4 brazed plate heat exchanger manufactured by Cetetherm AB was selected. The heat exchanger specifications are given in Table 5.

Pump and pipe

The cycle length of pipe for the secondary loop is around 110 m. The pressure head at the pipe end is kept at 2 bar. The amount of pressure loss in heating system components varies from one specification to another. The calculation assumes one radiator in each room. The calculation assumes pressure losses as shown in Table 6. Figure 6 shows the variations of pump power requirements with pipe diameter. The pipe diameter was selected to be a standard 0.025 m pipe, commonly available since the pump power does not decrease much as we increase the diameter further as shown in Figure 5. The corresponding pump power requirement was found to be 148 W.

TABLE 6: Pressure losses in heating system components

Component	No. of components	Pressure loss
Heat exchanger	1	20 kPa
Radiator	10	0.5 kPa
Radiator valve	10	10 kPa

Valve

Valves are used for switching and control of flow in the piping system to the radiator. The radiator valves can be of thermostatic type or manual. Thermostatic valves can be of two types. The first type controls the flow rate of hot water in accordance to the room temperature. The other type of thermostatic valves controls the flow rate in accordance to the return water temperature. On the other hand, manual valves need to be operated by human effort for controlling the flow rate depending upon the heating requirements. Thermostatic valves controlling the flow rate according to the return water temperature were used in the present design.

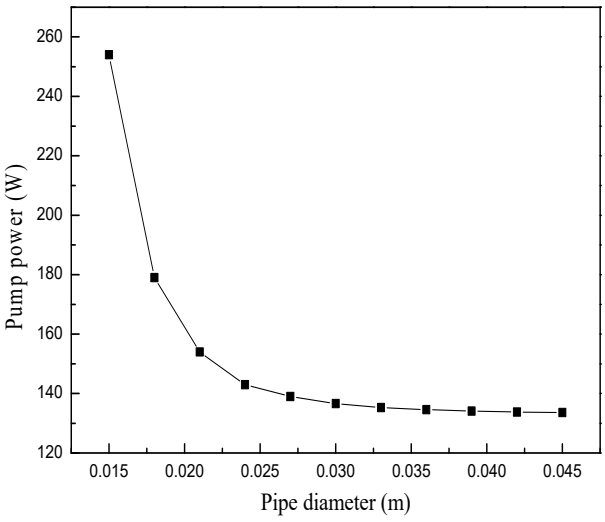

FIGURE 6: Variation of pump power with pipe diameter

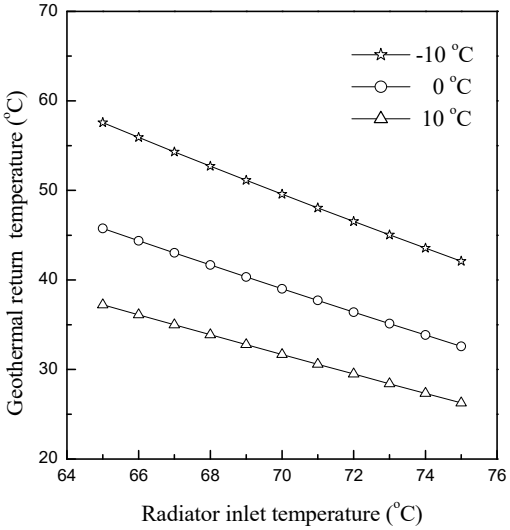

FIGURE 7: Variations of geothermal return temperature with radiator inlet temperature

5.2 Analysis

In order to have an optimized heating system, low temperature of the geothermal fluid exiting the heat exchanger is required, signifying high heat exchange in the radiator. Figure 7 shows the variation of geothermal outlet temperature from the heat exchanger at different radiator inlet temperature at three different ambient temperatures. Two important conclusions can be drawn from the graph, also reported in the literature (Karlsson and Ragnarsson, 1995). The first is the decrease in the geothermal fluid outlet temperature with an increase in the radiator inlet temperature. This is due to the fact that for a constant heat load, the logarithmic temperature difference remains constant for which the radiator outlet temperature decreases for a given increase in inlet temperature. Radiator inlet temperature is decided by the pinch point difference at the heat exchanger's geothermal water inlet. The second important conclusion is the increase in the geothermal fluid exit temperature with a decrease in ambient temperature. As the ambient temperature decreases, the heat load increases which causes an increase in the logarithmic temperature difference. For a constant inlet temperature, the outlet temperature from the radiator increases for a given increase in the logarithmic temperature difference. The increase in the geothermal fluid exit temperature with a decrease in ambient temperature results in a decrease in efficiency of the heating system with concerns about heat wastage at lower ambient temperatures.

Figure 8 shows the variation of the first and second laws of efficiency for room heating with ambient temperature. With the increase in ambient temperature, the first law of efficiency increases. Increase in the ambient temperature causes the radiator exit temperature to decrease as explained before. Decrease in the outlet temperature causes high heat removal per unit mass from the hot fluid passing through the radiator, with a subsequent increase in efficiency. The second law of efficiency also increases with ambient temperature as the exergy removal per unit mass through hot fluid increases with a decrease in the radiator outlet temperature. The increase in exergy removal from the hot fluid is then offset by a decrease in the exergy output as the reference temperature approaches the mean radiator temperature, hence causing the second law of efficiency to decrease.

The heating system was simulated by parallel additions of heat storage using phase change material for different ambient temperatures and for different time durations of the heat storage process in the phase change material. The storage material mass and other physical properties were kept constant during the analysis.

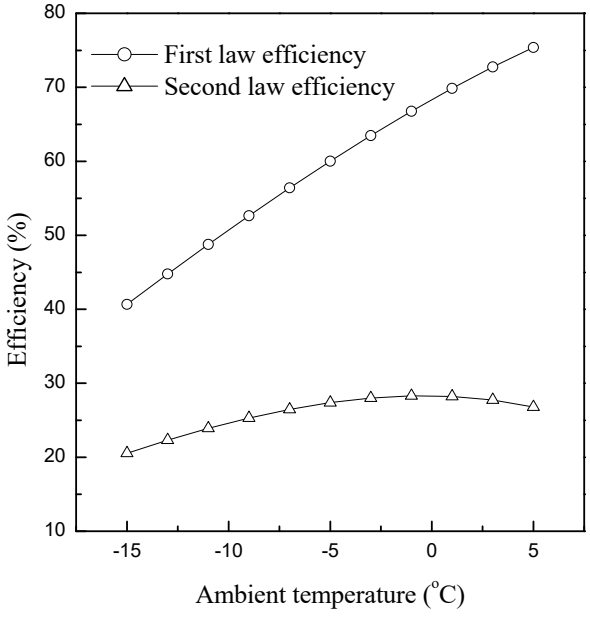

FIGURE 8: Variation of thermal efficiencies with ambient temperature

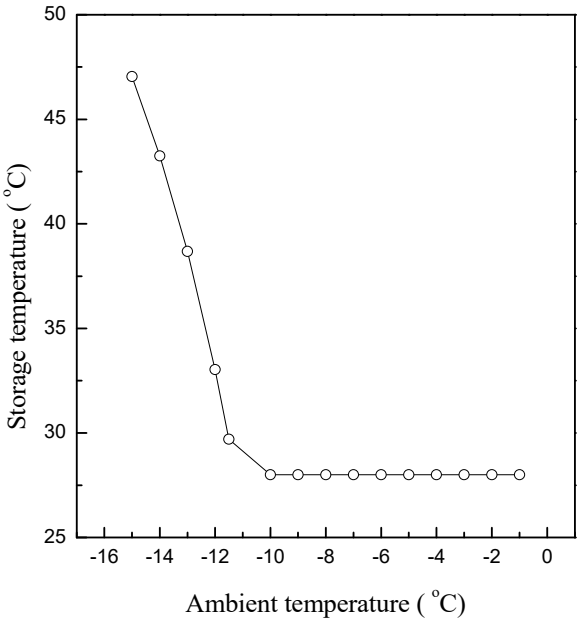

FIGURE 9: Variation of storage temperature with ambient temperature after an hour of operation

Figure 9 shows the variation of storage temperature with ambient temperature after an hour of the heat transfer process. It was found that at lower ambient temperature, heat gained by the phase change material was high enough that the phase change material was above the transition temperature earlier than expected. This occurred because of the high temperature and mass flow rate of the geothermal fluid at the storage inlet. With an increase in the ambient temperature, the heat exchanger or storage inlet temperature and mass flow rate of the geothermal fluid decreased causing a smaller heat transfer rate between the geothermal fluid and the phase change material. This caused the phase change material to remain in the transition stage after the same interval of time as that for a lower temperature.

Figure 10 shows the variation of heat transferred for different ambient temperatures after an hour of the heat storing process, keeping all other parameters constant. With the increase in ambient temperature, heat input from the geothermal fluid decreased. This occurred due to low geothermal fluid exit temperature at the heat exchanger exit. The required mass flow rate of the geothermal fluid also decreased with the increase in ambient temperature which also caused a decrease in the heat input from the geothermal fluid. Room heat load showed a continuous decrease as the ambient temperature increased. The amount of heat gained by phase change storage was higher at lower temperature and decreased with an increase in the ambient temperature. At lower ambient temperature, the phase change material was above the transition stage. The amount of heat stored was high, as the mass flow rate of the geothermal fluid at lower temperature also added to the high heat storage. The amount of heat stored at lower ambient temperature was the sum of latent heat of the material and the sensible heat stored at the storage temperature of the material at that time period. The exergy changes also showed similar trends as shown in Figure 11. Figures 10 and 11 show significant contribution made by phase change storage in energy savings at low ambient temperature. The graphs show that the energy and exergy stored were small in comparison to the total input but were significant in comparison to the room heat load.

Thermodynamic analysis of the storage system was done for different periods of charging, assuming -10°C ambient temperature. Figure 12 shows the variation of phase change material storage temperature with time during charging. The initial temperature of the phase change material was assumed to be equal to the room temperature. With an increase in the storage time, storage temperature increased until the transition temperature occurred. Since the temperature difference between the heat source fluid and the storage temperature was high, heat transferred rapidly causing a rapid increase in the storage

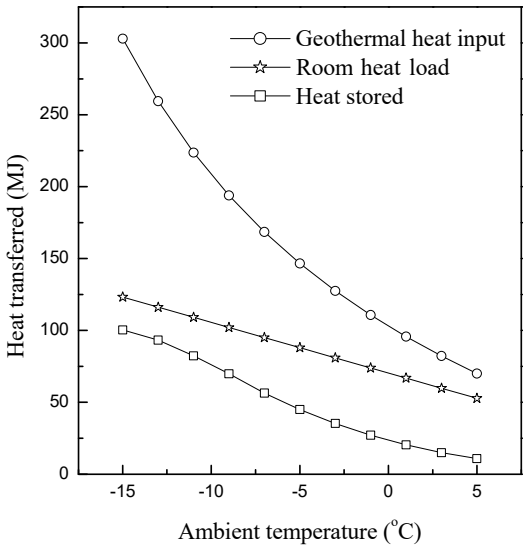

FIGURE 10: Variation of heat transfer with ambient temperature after an hour of operation

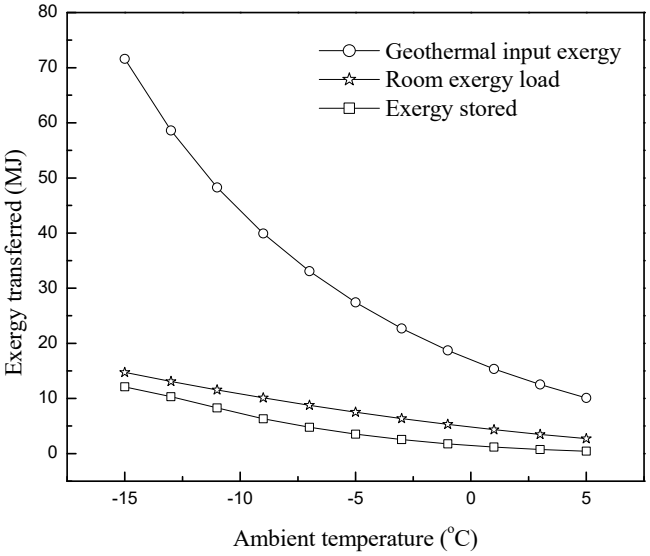

FIGURE 11: Variation of exergy transferred with ambient temperature after an hour of operation

temperature. On reaching the transition temperature heat transfer occurred at a constant temperature until the latent heat of the material was absorbed. After the transition phase was over, the storage temperature again started to increase, first at a high rate and then more slowly as the storage temperature became closer to the heat transfer fluid inlet temperature.

Figure 13 shows the variation of total heat transferred by the geothermal heat source fluid, room heat load and stored heat with time. With an increase in time duration, the total room heat increased constantly as the ambient temperature was fixed, hence, a fixed heat load. Total geothermal heat input from geothermal heat source also increased linearly since for a constant room heat load mass, the flow rate of the geothermal fluid also remained constant and the inlet hot fluid temperature was also fixed. The constant increase is reflected by the constant slopes of the geothermal heat input and room heat load in Figure 13. On the other hand, the total heat stored increased constantly till the transition stage was complete and then increased at a lower rate till the total heat stored became constant. The total heat

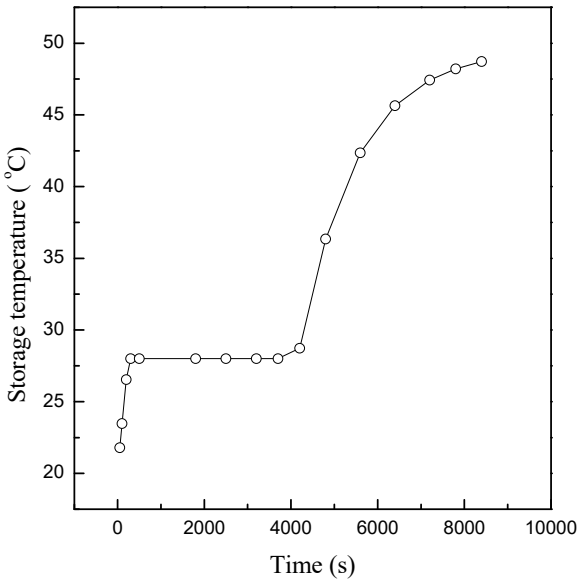

FIGURE 12: Variation of storage temperature with time at - 10°C ambient temperature

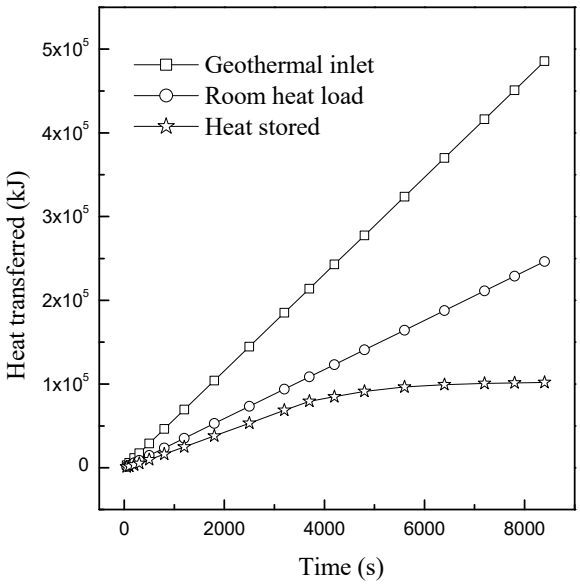

FIGURE 13: Variation of total heat transferred with time at - 10°C ambient temperature

stored showed a constant slope during the latent heat absorption. After that, sensible heat storage started taking place and the rate of heat storage decreased as the storage temperature started approaching the heat source fluid temperature. It can be seen from the graph that the room heat load requirement was much smaller than the total heat input from the geothermal fluid. The addition of a phase change storage system increased significantly the heat savings compared to the room heat load requirement. The significant amount of heat stored could be enough to satisfy the heat load requirement during the daytime when the heat load is less.

Figure 14 shows the variation of total exergy stored in the phase change material with time. The initial phase of the storage process showed a constant increase in exergy accumulation in the phase change storage process. This exergy accumulation process increased constantly until latent heat storage took place. After the phase transition was complete, sensible heating started. The rate of exergy accumulation in the phase change storage material then started decreasing as the storage temperature approached the geothermal fluid inlet temperature.

Figure 15 shows the variation of fractional exergy stored as a function of the fractional heat stored. The initial and end part of the graph represents heat storage due to sensible heating and the middle constant range represents latent heat storage. It is seen from the graph that major exergy accumulation took place in the latent heat change process and sensible heating of the phase change material did not contribute much to exergy storage. Hence, it can be concluded from the graph that latent heat storage makes more of a contribution to heat storage than sensible heat.

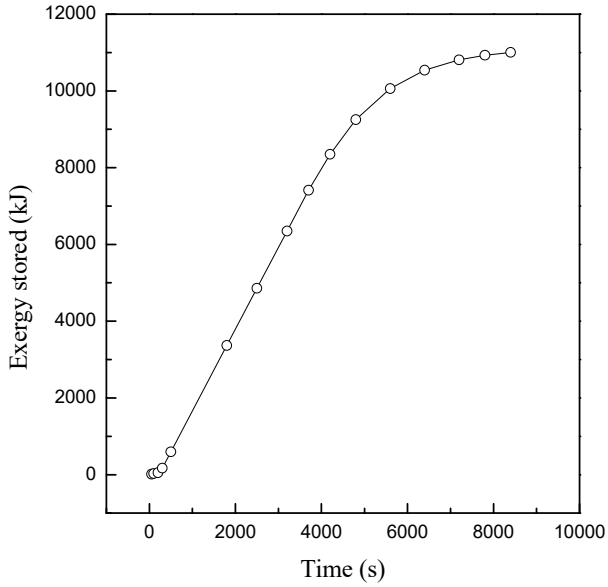

FIGURE 14: Variation of total exergy stored with time at - 10°C ambient temperature

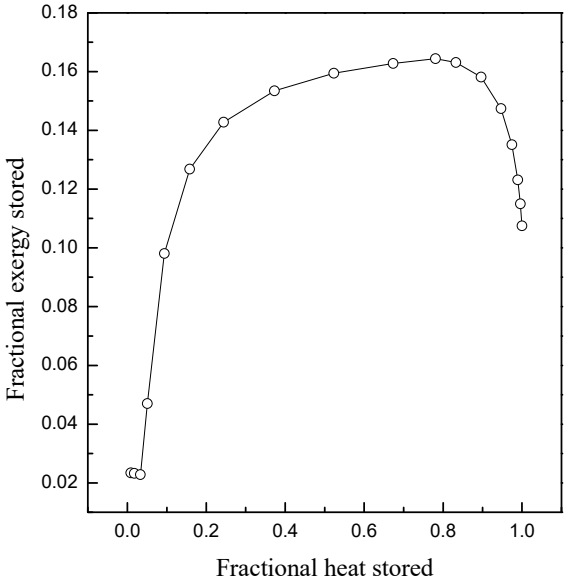

FIGURE 15: Variation of fractional exergy stored with fractional heat stored

Figure 16 shows the variation of cost flow rate per unit exergy ($/kJ/hr) at different ambient temperatures. The inlet cost flow rate of the geothermal fluid is associated with that of the well and pumping costs. Since the well cost varies from place to place, the present analysis assumed a well cost of 0.5 million USD and 0.1 USD/kWh for the pumping cost with a total required head of 200 m from pump and an annual 7000 hours of operation. The discharge from the well was assumed to be 12 kg/s. The exergy flow rate from a geothermal fluid depends upon the ambient temperature. With an increase in ambient temperature, exergy per unit mass flow rate of geothermal fluid decreases as the reference temperature increases. Also the increase in ambient temperature causes a decrease in the mass flow rate through the well as the heat load decreases. These two factors cause the cost flow rate of the geothermal fluid to increase with ambient temperature. The cost flow rate of exergy supplied by radiators to a room increases with ambient temperature. As the ambient temperature increases, the heat load required

decreases causing the required exergy flow rate to decrease. The decrease in the exergy flow rate does not affect the purchase cost associated with the heat exchanger and radiator since the size of the equipment depends upon the design conditions for the minimum ambient temperature. Similar variations were found for the cost flow rate of exergy stored in the phase change storage system. The increase was found to be greater at higher ambient temperature. This occurs because as the ambient temperature increases, the heat exchanger exit temperature and mass flow rate decrease causing less exergy flow rate at the heat exchanger exit. The decrease in the exergy flow rate causes an increase in the cost flow per unit exergy as the purchasing cost remains the same as that for minimum ambient design conditions. An important observation from the graph is the difference in cost flow rates of the radiator heating and the stored exergy. It can be seen from the graph that the cost flow rate of stored exergy is lower than the radiator heating at lower ambient temperature. Since with the increase in ambient temperature the cost flow rate of the radiator heating increases, the amount of exergy stored at lower temperature with a low cost flow rate could be used at higher temperatures, resulting in cost savings.

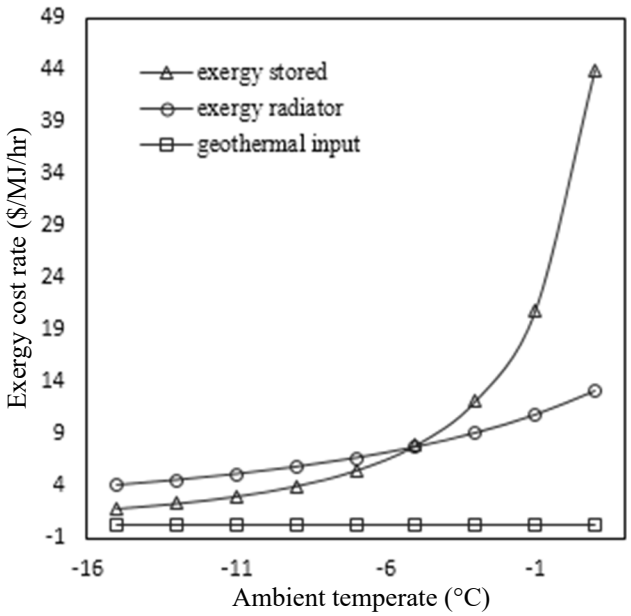

FIGURE 16: Variation of exergy cost flow rate per unit exergy with ambient temperature

Table 7 shows the exergy and cost flow rate per unit exergy at different state points in the combined heating and storing system at -5°C ambient temperature. The values of the cost flow rates per unit exergy show that each system, including a geothermal well and pumping, a heating system and a heat storage system, makes a significant contribution to the overall product cost rate, that is the cost of room heating and storing exergy. Also the low value of exergy storage cost in comparison to room heating using a radiator system at higher temperature shows the advantage of storing exergy at low ambient temperature.

TABLE 7: Exergy and cost flow rates at -5°C ambient temperature

State points	Exergy flow rate (kW)	Cost per unit exergy (USD MJ^{-1} hr^{-1})
Geothermal inlet	7.61	0.32
Storage inlet	2.73	0.32
Storage exit	1.6	0.32
Radiator inlet	6.04	0.69
Radiator exit	1.77	0.69
Room heating	2.08	7.83
Storage	0.69	7.98

6. CONCLUSIONS

Thermodynamic and exergoeconomic analysis of space heating using geothermal energy was done for a building in Chumathang, India. Due to the extreme cold conditions and poor insulation of the houses, the heat load requirement is high as calculated. The cost involved with drilling and pumping also

contributes to the total cost for space heating. The cost becomes significant when the flow rate requirement is high due to high heat load requirements.

Variations of heating system efficiency with ambient temperature were studied. Heating system efficiency was found to be low at lower ambient temperature. Hence, thermal losses become significant at lower temperatures.

A parallel combination of a phase change storage system with a heating system was studied. Heat supply to the storage system was provided from heat exiting the heat exchanger. Thermodynamic studies of the heat storage process at different times and ambient temperatures were done. Higher heat storage was observed at low ambient temperature. The rate of exergy storage during the latent heat transition period was found to be larger than for sensible heat storage. A sufficient amount of exergy was stored during the charging period at low temperature which could be used to fulfil the daytime heat load requirements.

Exergoeconomic analysis of the combined heating and storage system was done. At low ambient temperature, the cost flow rate of exergy storage was found to be lower than the radiator heating cost flow rate. For the assumed value of investment cost rates, heat storage using phase change material was found to be more economical than radiator heating till -5°C. Another important conclusion drawn was the increase in the cost flow rate of radiator heating exergy with ambient temperature. The usage of exergy storage at low ambient temperature for heating at higher ambient temperature could make significant contributions in cost savings.

Thermodynamic and exergoeconomic analysis of heating using geothermal energy in combination with a phase change storage system was done. Parametric analysis was done using a selected storage phase change material. Results showed both thermodynamic and exergoeconomic feasibility and scope for optimization. Future work must concentrate on the application of phase change materials with different transition temperatures and their combinations in order to optimize the storage process both thermodynamically and thermoeconomically.

ACKNOWLEDGEMENTS

I thank the United Nations University, the Indian Institute of Technology, Mandi, and the Government of Himachal Pradesh for giving me the opportunity to attend this program. My sincere gratitude goes to Dr. Ingvar Birgir Fridleifsson, Mr. Lúdvík S. Georgsson, Ms. Málfrídur Ómarsdóttir, Mr. Ingimar Gudni Haraldsson, Ms. Thórhildur Ísberg, Mr. Markús A.G. Wilde and Ms. Rósa S. Jónsdóttir for all their guidance and services.

I wish to express my sincere thanks to my supervisor Dr. Árni Ragnarsson and my teachers Dr. P. Anil Kishan, Dr. Sateesh Gedupudi, Dr. Ashan Absar, Prof. B.N Banergee and Prof. Deepak Khemani. I would like to thank my parents and elder brother. They were always supporting me and encouraging me with their best wishes. I also place on record my sense of gratitude to one and all who, directly or indirectly, have lent their helping hand in this venture.

Above all, I am grateful to The Almighty God for enabling me to complete my geothermal training Programme.

NOMENCLATURE

A_{exp} = area exposed (m^2);
A_{HX} = area of heat exchanger (m^2);
A_R = radiator area (m^2);
$c_{in,i}$ = inlet flow cost per unit exergy (\$/kJ);
$c_{out,i}$ = outlet flow cost per unit exergy (\$/kJ);
$c_{Q,i}$ = heat flow cost per unit exergy (\$/kJ);
$c_{w,i}$ = work flow cost per unit exergy (\$/kJ);
$\dot{C}_F$ = fuel cost flow rate (\$/s);
$\dot{C}_{g,in}$ = geothermal inlet cost flow rate (\$/s);
$\dot{C}_{g,out}$ = geothermal outlet cost flow rate (\$/s);
$\dot{C}_{heating}$ = heating cost flow rate (\$/s);
$\dot{C}_{HX,in}$ = heat exchanger inlet exergy cost flow rate (\$/s);
$\dot{C}_{HX,out}$ = heat exchanger outlet exergy cost flow rate (\$/s);
$\dot{C}_p$ = product cost flow rate (\$/s);
$\dot{C}_{R,out}$ = radiator outlet exergy cost flow rate (\$/s);
$\dot{C}_{R,in}$ = radiator inlet exergy cost flow rate (\$/s);
$\dot{C}_{storage}$ = storage exergy cost flow rate (\$/s);
C_a = specific heat capacity of air (kJ/kgK);
$C_{R,f}$ = specific heat capacity of radiator fluid (kJ/kgK);
$C_{g,f}$ = specific heat capacity of geothermal fluid (kJ/kgK);
C_l = specific heat capacity of phase change material in liquid phase (kJ/kg);
C_{pcm} = latent heat capacity of phase change material (kJ/kg);
C_s = specific capacity of phase change material in solid phase (kJ/kg);
D_h = hydraulic diameter (m);
D_{inner} = inner diameter (m);
D_{outer} = outer diameter (m);
e = exponent for cost;
D_p = pipe diameter (m);
r_p = pipe roughness factor (m);
f = friction factor;
g = acceleration due to gravity (m/s^2);
h = convective heat transfer coefficient ($W/m^2 K$);
h_m = convective heat transfer coefficient of storage side ($W/m^2 K$);
h_g = convective heat transfer coefficient of geothermal fluid side ($W/m^2 K$);
h_f = convective heat transfer coefficient of fluid flowing side ($W/m^2 K$);
h_R = convective heat transfer coefficient of radiator fluid side ($W/m^2 K$);
$h_{geo,in}$ = specific enthalpy of geothermal inlet fluid (kJ/kg);
h_o = specific enthalpy of fluid at reference state (kJ/kg);
h_l = head loss (m);
h_s = static head required (m);
H = latent heat capacity of storage material (kJ/kg);
i = interest rate per annum (%);
I = cost of equipment (\$);
I_r = cost of reference equipment (\$);
k = bending loss coefficient;
L_p = length of pipe (m);
L_s = length of phase change storage (m);
$LMTD_{HX}$ = logarithmic mean temperature difference of heat exchanger (K);

$LMTD_R$ = logarithmic mean temperature difference of radiator/room (K);
$LMTD_{R,des}$ = logarithmic mean temperature difference of radiator/room at design conditions (K);
$\dot{m}_f$ = mass flow rate (kg/s);
$\dot{m}_{geo}$ = geothermal water mass flow rate (kg/s);
$\dot{m}_{rad}$ = radiator fluid mass flow rate (kg/s);
M_{pcm} = phase change material mass (kg);
N = number of years of operation;
P_{pump} = pump power (kW);
$\dot{Q}_{des}$ = design heat load (kW);
$\dot{Q}_T$ = heat load (kW);
$\dot{R}_{HX}$ = resistance due to fouling in heat exchanger (m^2 K/W);
$s_{geo,in}$ = geothermal water inlet entropy (kJ/K);
s_o = reference state entropy (kJ/K);
S = size of equipment;
S_r = size of reference equipment;
t = time (s);
T = temperature (K);
T_o = reference ambient temperature (K);
T_{amb} = ambient temperature (K);
T_{des} = design ambient temperature (K);
T_l = final temperature of the phase change material (K);
T_b = initial temperature of the phase change material (K);
T_m = temperature in transition phase (K);
T_{rad} = mean radiator temperature (K);
T_{room} = room temperature (K);
$T_{R,in}$ = radiator fluid inlet temperature (K);
$T_{R,out}$ = radiator fluid outlet temperature (K);
$T_{g,in}$ = geothermal water inlet temperature (K);
$T_{g,out}$ = geothermal water outlet temperature (K);
U_{HX} = heat exchanger overall heat transfer coefficient (W/m^2 K);
U_R = radiator overall heat transfer coefficient (W/m^2K);
U_s = storage system overall heat transfer coefficient (W/m^2 K);
v_f = fluid velocity (m/s);
$\dot{W}_i$ = rate of work for i^{th} component (kW);
x_{HX} = thickness of heat exchanger plate (m);
$Y_{q,room}$ = exergy quality factor;
$\dot{Z}^{Cl}$ = levelized capital cost ($/s);
$\dot{Z}^{OM}$ = levelized operation and maintenance cost ($/s);
$\dot{Z}_{HX}$ = total cost rate of heat exchanger ($/s);
$\dot{Z}_{storage}$ = total cost rate of storage system ($/s);
$\dot{Z}_R$ = total cost rate of radiator ($/s);
ρ_f = density of fluid (kg/m^3);
ρ_a = density of air (kg/m^3);
v_f = velocity of fluid (m/s);
β = annual operation and maintenance cost (%);
μ_f = dynamic viscosity of fluid (N s/m^2);
θ_b = dimensionless temperature at initial state;
θ_e = dimensionless exit temperature of geothermal fluid;
θ_i = dimensionless inlet temperature of geothermal fluid;
θ_l = dimensionless temperature in liquid phase;
θ_m = dimensionless phase transition temperature;

θ_s = thermal storage temperature;
$\dot{\varepsilon}_D$ = exergy destruction rate (kW);
$\dot{\varepsilon}_F$ = fuel exergy flow rate (kW);
$\dot{\varepsilon}_L$ = exergy loss rate (kW);
$\dot{\varepsilon}_P$ = product exergy flow rate (kW);
$\dot{\varepsilon}_{Q,i}$ = exergy flow rate due to heat flow in i^{th} component (kW);
$\dot{\varepsilon}_{out,i}$ = outlet exergy flow rate from i^{th} component (kW);
$\dot{\varepsilon}_{g,in}$ = geothermal water inlet exergy flow rate (kW);
$\dot{\varepsilon}_{g,out}$ = geothermal water outlet exergy flow rate (kW);
$\dot{\varepsilon}_{HX,out}$ = exergy flow rate from heat exchanger outlet (kW);
$\dot{\varepsilon}_{in,i}$ = inlet exergy flow rate to i^{th} component (kW);
$\dot{\varepsilon}_{room}$ = exergy required for heating (kW);
$\dot{\varepsilon}_{rad}$ = exergy given by the radiator (kW);
$\dot{\varepsilon}_i$ = exergy flow rate at i^{th} component (kW);
$\dot{\varepsilon}_{geo}$ = exergy given by the geothermal fluid (kW);
$\dot{\varepsilon}_{stored}$ = exergy stored in the PCM (kW);
λ_f = thermal conductivity of fluid (W/mK);
λ_s = thermal conductivity of heat storage material (W/mK);
λ_{surf} = thermal conductivity of wall material (W/mK);
λ_{HX} = thermal conductivity of heat exchanger plate (W/mK);
η_{pump} = efficiency pump (%);
Ω = dimensionless time.

REFERENCES

Abhat, A., 1983: Low temperature latent heat thermal energy storage: heat storage materials. *Solar Energy, 30,* 313–332.

Adebiyi, G.A., and Russell, L.D., 1987: Second law analysis of phase-change thermal energy storage systems. *Proceedings of the ASME, WA-HTD-80, Boston, MA*, 9-20.

Anon, 1977: *DIN 4703 Part 3. Heat transport of bodies at room temperature* (in German). Beuth Verlag, Berlin, Germany.

Bejan, A., 1996: Entropy generation minimization: The new thermodynamics of finite size devices and finite time processes. *J. Applied Physics, 79,* 1191-1218.

Bejan, A., Tsatsaronis, G., and Moran, M., 1996: *Thermal design and optimization*. John Wiley & Sons, NY, 542 pp.

Bjurstrom, H., and Carlsson, B., 1985: An exergy analysis of sensible and latent heat storage. *J. Heat Recovery Systems, 5*, 233-250.

Boehm, R.F., 1987: *Design and analysis of thermal systems,* John Wiley and Sons, NY, 259 pp.

Budaiwi, I.M., 2011: Envelope thermal design for energy savings in mosques in hot humid climate. *J. Building Performance Simulation*, ***4***, 49-61.

Carlos, J.S., and Nepomuceno, M.C.S., 2004: A simple methodology to predict heating load at an early design stage of Dwellings. *Energy Conversion and Management*, *45*, 1597-1615.

Cooper, J.R., and Dooley, R.B., 2007:*Revised release on the IAPWS industrial formulation 1997 for the thermodynamic properties of water and steam*. IAPWS, Lucerne, Switzerland, 49 pp.

Crawley, D.B., Hand, J.W., Kummert, M., and Griffith, B.T., 2008: Contrasting the capabilities of building energy performance simulation programs. *Building and Environment*, *43,* 661-673.

El-Dessouky, H., and Al-Juwayhel, F., 1997: Effectiveness of a thermal energy storage system using phase change materials. *Energy Conversation and Management, 38*, 601-617.

Farid, M.M., Khudhair, A.M., Razack, S.A.K., and Al-Hallaj, S., 2004: A review on phase change energy storage: materials and applications. *Energy Conversion and Management, 45*, 1597-1615.

Hepbasli, A., 2010: A review on energetic, exergetic and exergoeconomic aspects of geothermal district heating systems (GDHSs). *Energy Conversion and Management, 51*, 2041-2061.

IEA ECBCS Annex 37, 2000: *Low exergy systems for heating and cooling of buildings. Annex 37, Conservation in buildings and community systems*. VTT, webpage: *www.vtt.fi.*

Incropera, F.P., Dewitt, D.P., Bergman, T.L., Lavine, A.S., and Middleman, S., 2007: *Fundamentals of heat and mass transfer: an introduction to mass and heat transfer* (6thed.). John Wiley and Sons Inc., NY, 1720 pp.

Jingyana, X., Juna, Z., and Na, Q., 2010: Exergetic cost analysis of a space heating system. *Energy and Buildings, 42*, 1987–1994.

Kalema, T., and Pylsy, P., 2008: Accuracy of the calculation of heating and cooling energy needs in Nordic conditions. *Proceedings of the 8th Symposium on Building Physics in the Nordic Countries, Copenhagen*, 535–542.

Karlsson, Th., and Ragnarsson, Á., 1995: Use of very low temperature geothermal water in radiator heating system. *Proceedings of the World Geothermal Congress 1995, Florence, Italy*, 2193-2198.

Keçebaş, A., 2013: Effect of reference state on the exergoeconomic evaluation of geothermal district heating systems. *Renewable and Sustainable Energy Reviews, 25*, 462-469.

Marshall, R.J., Lozowski, D., Ondrey, G., Torzewski, K., and Shelley, S.A., (eds.) 2009: Marshall and Swift cost index. *Chemical Engineering Magazine*, *February*, 64 pp.

Meester, B.D., Dewulf, J., Verbeke, S., Janssens, A., and Langenhove, H.V., 2009: Exergetic life cycle assessment (ELCA) for resource consumption evaluation in the built environment. *Build Environment, 44,* 11-17.

Mirsadeghi, M., Cóstola, D., Blocken, B., and Hensen, J.L.M., 2013: Review of external convective heat transfer coefficient models in building energy simulation programs: Implementation and uncertainty. *Applied Thermal Engineering, 56*, 134-151.

Moran, M.J., and Shapiro, H.N., 2007: *Fundamentals of engineering thermodynamics*. John Wiley and Sons, NY, 944 pp.

Oktay, Z., and Dincer, I., 2009: Exergoeconomic analysis of the Gonen geothermal district heating system for buildings. *Energy and Buildings, 41*, 154-163.

Razdan, P.N., Agarwal, R.K., and Singh, R., 2008: Geothermal energy resources and its potential in India. *e – J. Earth Science India, 1,* 30-42.

Saito, M., and Shukuya, M., 2001: The human body consumes exergy for thermal comfort. *LowExNews, 2*, 6-7.

Shukuya, M., and Komuro, D., 1996: Exergy–entropy process of passive solar heating and global environmental systems. *Sol Energy, 58*, 25-32.

Yanadori, M., and Masuda, T., 1989*:* Heat transfer study on a heat storage container with phase change materials: Part 2. *Solar Energy*, *42*, 27-34.

Yildiz, A., and Gungör, A., 2009: Energy and exergy analyses of space heating in buildings. *Applied Energy, 86,* 1939-1948.